

PECULIARITIES OF CHARGE TRANSPORT IN A SEMICONDUCTOR GAS DISCHARGE ELECTRONIC DEVICES

E. KOÇ¹, M. ÇİVİ¹ and B.G. SALAMOV^{1,2}

¹Physics Department, Faculty of Arts and Sciences,
Gazi University, 06500 Ankara, Turkey

²National Academy of Science, Institute of Physics,
AZ-1143 Baku, Azerbaijan

The memory effect in planar semiconductor gas discharge system (SGDS) at different pressures (15-760 Torr) and interelectrode distance (60-445 μm) were experimentally studied. The study was performed on the bases of current-voltage characteristic (CVC) measurements with the time lag of several hours of afterglow periods. The influence of the active space-charge remaining from previous discharge on the breakdown voltage (U_B) has been analyzed using the CVC method for different conductivity of semiconductor GaAs photocathode. On the other hand, the CVC data for subsequent dates present a correlation of memory effect and hysteresis behaviour. The explanation of such relation is based on the influence of long-lived active charges on the electronic transport mechanism of semiconductor material.

1. INTRODUCTION.

The interest in studying memory effect with non-linear CVC in semiconductor gas discharge electronic devices with semi-insulating (SI) GaAs cathode is experimentally studied due to the necessity of extending knowledge in the field of semiconductor and gas-discharge physics and to help solve practical problems associated with the use of this kind of discharge in technical devices. Semiconductor gas discharge IR image converters with GaAs cathodes have found numerous applications, especially in the registration of IR images [1,2]. The memory effect is the phenomenon that some active species survive the long τ (i.e. the time elapsed after the discharge has been turned off to the application of the new voltage pulse) and affect subsequent breakdown. This phenomenon had been observed when monitoring memory curves for rare gases, H_2 and N_2 , for τ interval from 3 s to 24 h [3,4]. The τ value depends on the gas type. Physical interpretation of the memory effect was not given, other than it is a consequence of the presence of some unknown long living metastable states in the afterglow formed by the previous discharge. In this study we investigate the influence of products of a low-pressure atmospheric air glow discharge on the next breakdown and CVC. We discuss the possible causes of the observed memory effects and some practical suggestions on how to deal with them are given (ionization process, measurement of the pre-breakdown current). This effect is not observed in gas discharge gap with two metallic electrodes [5] conducted by us. So, the memory effect is due to the GaAs cathode. The memory effect, as a function of the parameters of the preceding discharge, has been observed for a number of different cathode materials, several gases and various experimental set-ups [3]. On the other hand, non-linear characteristic of SI GaAs cathode which is electrically interfaced/coupled with gas discharge structure is also investigated. The presence of the NDC in SI GaAs cathode is associated with instabilities of a homogeneous steady state produced by spatial fluctuations in the electric field or in the carrier density. Since the high electric-field domains in SI GaAs are caused by electron trapping by EL2 [6].

2. EXPERIMENTAL.

A schematic of the SGDS with a GaAs cathode is shown in Fig.1. The GaAs photocathode characterized by high-resistivity ($\rho \sim 8 \times 10^8 \Omega\text{cm}$). The experiments were carried out with the cathode plate (2) made of a SI n-type GaAs [7]. The GaAs crystal plate with a [100] surface was cut from single-crystal ingot grown by the LEC method [7,8]. The diameter and the thickness of the cathode were 36 mm and 1 mm, respectively. To realize the systems shown in Fig.1, the external surface of the photocathode (2) was covered with a Au layer (1) of high conductivity, which is approximately 40 nm thick. Therefore, it is transparent to IR light with a transmission of about 10%. Opposite the semiconductor layer, there is a glass plate (6) that is covered with a transparent and conductive SnO_2 layer (5). The surface of the GaAs cathode was separated from a flat anode by an insulating mica sheet (4) with a circular aperture at its centre (3), the internal diameter of which determined the active electrode areas S of the gas gap ($S = 0.8, 10.2$ and 15.2 cm^2). The SnO_2 and the Au electrode are connected to the external electric circuit, which consists of a dc high voltage supply and a series load resistor R_l (10 k Ω) that is included to measure the current in the circuit. The space between the glass plate and the semiconductor is the gas layer. By applying a high voltage U_0 between the Au contact and the SnO_2 layer, a discharge is ignited in the gap. This corresponds to a discharge operating in the Townsend regime (this stable form of discharge is employed in the semiconductor gas discharge IR image converter [9,10] possessing linear CVCs). The size of the discharge gap d (60–445 μm) and the gas pressures p (0.1–70 Torr) were chosen so as to provide a rather bright DLE due to charge impact even at a low current density and thus resulting in a high efficiency of the emission process [8,11]. Constant voltage from the stabilized power supply ($U_0 = 50$ –1000 V) was applied to the SGDS. The minimum current registered by the recorder was 6.0×10^{-11} A. The illumination intensity L is varied in the range 10^{-6} – 10^{-2} Wcm^{-2} by the use of neutral density filters. The maximum illumination intensity is around $8 \times 10^{-2} \text{ Wcm}^{-2}$. All the experimental study was performed in atmospheric air and the measurements were carried out at room temperature.

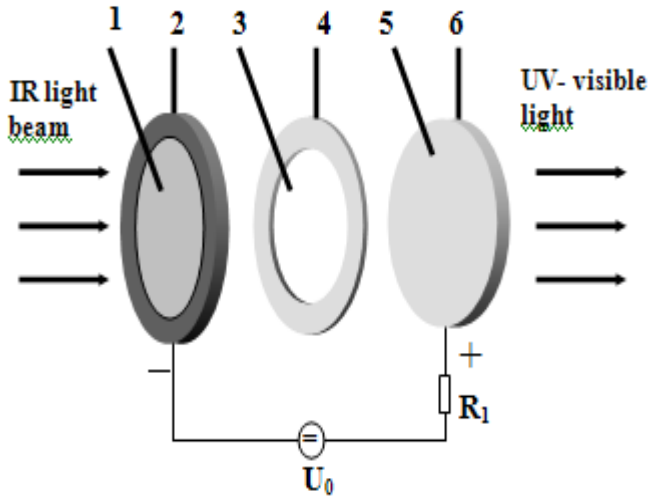


Fig.1. Scheme of the gas discharge cell: 1 – semi-transparent Au - contact; 2- GaAs cathode; 3 – gas discharge gap; 4– mica foil; 5- transparent conductive SnO₂ contact; 6 - flat glass disk.

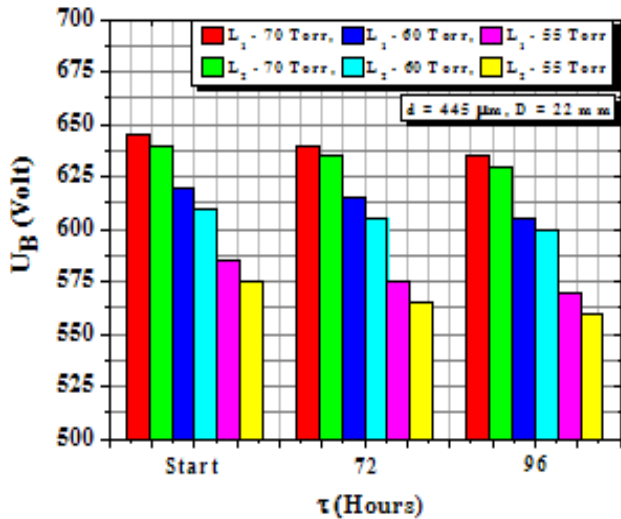


Fig.2. Time dependence of breakdown voltage U_B (start, 72 and 96 hours). System parameters, $p = 60 \text{ Torr}$, $d = 445 \mu\text{m}$, $D = 22 \text{ mm}$, for weak and strong illumination intensities L_1 and L_2 .

3. RESULT AND DISCUSSION.

We concentrate on a *dc* driven gas discharge explaining its *CVC* and different discharge modes. Also we analyze the behaviour of memory curves at different pressures in the aim of revealing of electrical transport mechanism. On the bases of these curves the influence of external illumination on the memory effect is also investigated. In this case, the procedure for post-breakdown current measurements was as follows: the voltage is applied to the *SGD* cell and the cell is moved towards the breakdown status under external illumination. After that, U_0 is switched on and during each second, increasing the U_0 value simultaneously. The minimum voltage value for which the electrical breakdown still appears can be considered as U_B . The dc voltage was increased at rate of 5 V/sec through each experiment. The time dependence of the U_B (i.e. influence of memory effect) for air-filled cell at different pressures (55, 60 and 70 Torr) is shown in Fig.2. Such a memory effect has been observed even for periods of

hundred hours ($\tau \approx 100 \text{ h}$). Larger memory effect influence results in lower U_B value. It can be concluded that value of U_B will be lower for lower pressure value. U_B depends on the rate of applied voltage increase U_0 and on the contact materials, cathode surface, cathode materials [12] and on the presence of *IR* illumination. It should be noted, that the U_B is lower when the cell is illuminated by *IR* light. The latter is in accordance with an earlier result that showed additional ionization in inter-electrode space decreases U_B [13]. Fig.2. present experimental data of electrical breakdown for different relaxation intervals τ . Naturally, when there are more active particles present in the discharge volume or on the cathode surface, there is a greater chance that one of them will initiate the discharge and hence the development of a discharge will be faster. Fig.2. show the influence of active species remaining from the previous discharge on the voltage range characterizing the U_B , we believe that the U_B values is decreased due to the accumulation charges on the cathode material which initiate U_B at lower values in comparison to the previous *CVC* measurement.

Fig.3 shows the *CVCs* for post-breakdown photocurrent measured at different dates. After the pumping down the gap pressure to 60 Torr, then the dc feeding voltage was applied to the gap to measure stationary current for three different time intervals (start, 72 and 96 hours). The cell with high resistance ($R_{\text{sem}} = 8 \times 10^{10} \Omega$) semiconductor cathode, a current of $6 \times 10^{-11} \text{ A}$ was registered at $U_0 = 560 \text{ V}$ and starts to increase at $U_0 = 560 \text{ V}$ (this structure is the basic component of the *IR* image converter [4,14]). At this voltage the ionization of gas is initiated. In the cell with a semiconductor *GaAs* cathode, the transition from the low steady state current to high steady state current takes place locally at different regions of the semiconductor independently, so the current increases fluently. Fig.3. shows the *CVC* of the gas discharge cell in parallel-plane geometry with different conductivity, σ , of the semiconductor cathode, which was varied by accumulation of long lived active species particles, remained from the previous discharge in the interior of discharge cell or on surface semiconductor cathode (memory effect).

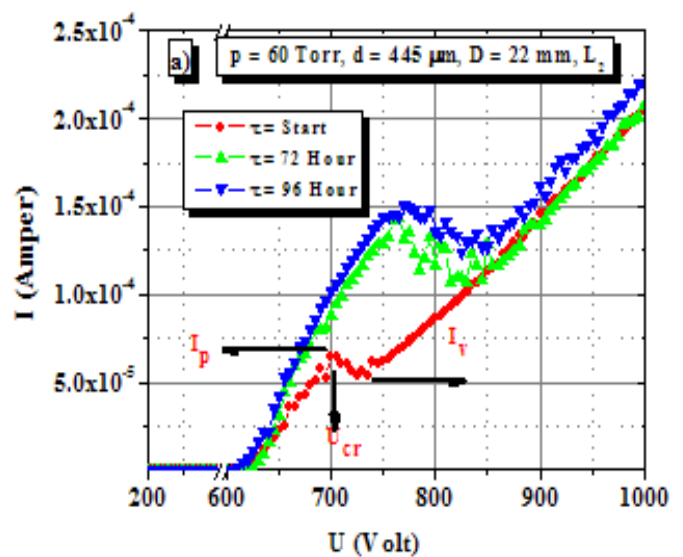


Fig.3. *CVCs* for discharge cell with *GaAs* cathode measured on different intervals; start, 72 and 96 hours, respectively. System parameters $d = 445 \mu\text{m}$, $D = 22 \text{ mm}$, $p = 44 \text{ Torr}$

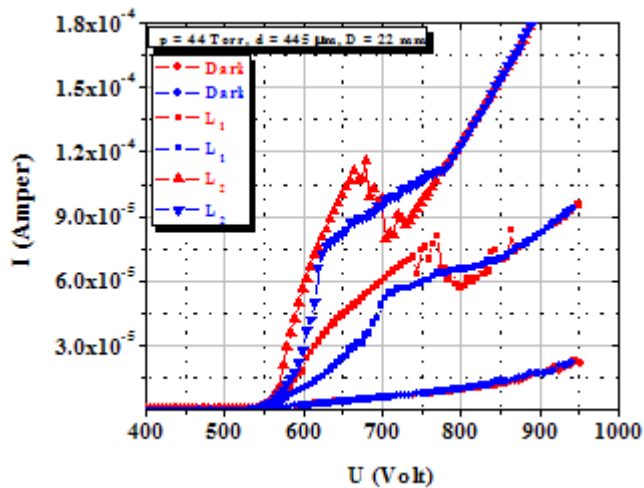


Fig.4. CVCs with N-shaped and hysteresis behaviour for discharge cell, red and blue color curves refer to forward increment and reverse decrement of U_0 on SGDS whilst GaAs cathode exposed to strong and weak illumination intensity and in darkness.

It is known [15] that light can induce a physical transformation of the centre in GaAs without modification of its electrical charge at 77 K. This effect, which arises on the so-called EL2 centre in GaAs [16], is explained by the existence of two states of these centres. The explanation of photocapacitance quenching of data and most memory effects in GaAs containing the O level certainly involves a centre with two states: one stable and another metastable. The physical parameters of these stable and metastable states are optical cross section, annealing and electrical de-excitation. This gives a very good phenomenological description of the experimental data coming from photocapacitance and photoconductivity. Thus, Vincent and co-workers proposed a physical model of photoelectric memory effect in GaAs [15], based on a large lattice relaxation.

On the other hand, the N-shaped I-V curves in Fig.3. are attributed to the EL2 center exists in the bulk material of SI GaAs cathode. The voltage range characterizing the onset of N-shaped I-V curves is termed as critical voltage U_{cr} , it shifts to higher U_{cr} values 700 V, 755 V and 770 V respectively for subsequent relaxation time. The current that corresponds to U_{cr} is called peak current (I_p) whereas the minimum current value at which the current start to ramp again is called valley current (I_V) (see the arrows in Fig.3). The experimental data in Fig.3 exhibits CVC with hysteresis behaviour between the three curves conducted at different intervals. We have experimentally observed that the hysteresis phenomena for different dates realized by charging/ discharging the surface state of semiconductor. Increasing surface charge state aids the extraction of carriers to the surface of semiconductor is enhanced as shown in our CVC curves for subsequent dates. Our experimental data show the interaction of accumulated active space-charge on the semiconductor cathode surface influence the nature of EL2 defects and electronic transport properties GaAs. Increasing surface charge state aids the extraction of carriers to the surface of semiconductor is enhanced as shown in our CVC curves for subsequent dates. The time dependence of peak and valley current (PVC) values is presented in Table 1 for subsequent relaxation time.

Table 1. Time dependent of critical voltage U_{cr} and PVC values at separate relaxation dates. System parameter: $p = 60$ Torr, $d = 445 \mu\text{m}$, $D = 22$ mm, illumination intensity L_2 .

Interval (Hours)	U_{cr} (V)	I_p (μA)	I_V (μA)
Start	700	0.065	0.053
72	755	0.144	0.108
96	770	0.151	0.127

The PVC values generally increase with time under strong illumination intensities L_2 . We believe that an inhomogeneous SI GaAs with the current flow localized in small regions of active electrode area causes the observed variations in peak voltages, multiple NDC regions, peak spreading and exponentially rising background current density J . SGDS are known to be complex nonlinear dynamic systems which exhibit current instabilities and self-organized formation of spatiotemporal patterns under the influence of strong electric fields [17,18]. Detailed study of pressure and illumination on CVCs effects are given in [19]. An N-shaped NDC is especially apparent at larger electrode spacing and smaller currents (see Fig.3). SI GaAs samples are also efficiently photosensitive [20] in the near IR range.

Depending on gas saturation of electrodes CVC hysteresis of various degree is observed. For pure electrode surfaces of low gas saturation it manifests itself negligibly. In this case current measurement process can influence CVC behaviour. In presence of oxide film CVC hysteresis is well pronounced. This might be caused by two reasons: local field resulting from the electric charge in the oxide film due to processes in pores and modifications of adsorbed layers influencing pressure in pores. Penetration and diffusion of the accumulated active particles from the surface into interior of semiconductor are realized especially when aided by electric field can modulate conductance. Fig.4. illustrates CVC with hysteresis curves peculiarities and non-equilibrium characteristics phenomena. Fig.4. also presents CVC hysteresis loop between forward and reverse driven feeding voltage at various conductivities of semiconductor cathode. The persistent large hysteresis points to the fact that localized nature of the surface state by charging and discharging these surface states, one can change the conductivity of the semiconductor, leading to the observed memory effect. Non-volatile memory effect in SI GaAs material was also observed in electrically

programmable read only memory with N -shaped CVC curves [17].

4. CONCLUSION.

We have presented the influence of active charged particles states remaining after long period $\tau \approx 100$ hours from the previous discharge in $SGDS$ experimentally. Our experimental results show that the recombination of metastable active particles in air survives up to several hours similar study for Ar , N_2 and H_2 described in [21]. The nonlinear CVC with hysteresis peculiarity in post-breakdown region is based on the mechanism of electron capture and emission from EL2 deep center defects in bulk of semiconductor material [17]. On the other side, the critical

voltage U_{cr} to onset N -shaped CVC is related to photoelectric memory effect [15] which is explained by the existence of two states (stable and metastable) of EL2 centers in the $SI GaAs$ material. The results obtained confirm the possibility to explain the total voltage/current effect based on processes occurring mainly in the cathode ports. These processes depend on the penetration of the external field into the pores, and the larger the distance between the electrodes, the deeper a constant, electric field reaches into the pores.

ACKNOWLEDGMENTS: This work is supported by the Gazi University BAP research projects 05/2008-13 and 05/2008-20.

-
- [1]. *B.G. Salamov, N.N. Lebedeva, K. Colakoglu and S. Altindal* 1998 *Imaging Sci. J.* 46 65
- [2]. *L.G. Paritskii and S.M. Rivkin* 1970 *Semiconductors* 4 764
- [3]. *M.M. Pejovic* 2004 *Phys. Plasmas* 11 3778–86
- [4]. *M.M. Pejovic, B.J. Mijovic and Dj.A. Bosan* 1984 *J. Phys. D: Appl. Phys.* 17 351
- [5]. *B.G. Salamov, N.N. Lebedeva, H.Y. Kurt, V.I. Orbukh. and E.Yu. Bobrova* 2006 *J. Phys. D: Appl. Phys.* 39 2732
- [6]. *R.M. Rubinger., de A.G. Oliveira, J.C. Bezerra, G.M. Ribeiro, W.N. Rodrigues and. M.V. Moreira B.,* 2000 *Phys. Rev. B* 15, 1
- [7]. *B.G. Salamov, A.A. Agasiev, N.N. Lebedeva, V.I. Orbukh, H.Y. Kurt and K. Colakoglu.* 2002 *J. Phys. D: Appl. Phys.* 35 716
- [8]. *B.G. Salamov* 2004 *Imaging Sci. J.* 52 225
- [9]. *B.G. Salamov, S. Ellialtioglu, B.Akinoglu, N.N. Lebedeva and L.G. Paritskii* 1996 *J. Phys. D: Appl. Phys.* 29 628
- [10]. *B.G. Salamov, S. Buyukakkas, M. Ozer and K. Colakoglu* 1998 *Eur. Phys. J. AP.* 2 275
- [11]. *B.G. Salamov, Ciftci Y Oztekin., K. Colakoglu* 2004 *IEEE Trans. Plasma Sci.* 32 2093 Part 2
- [12]. *H.Y. Kurt and B.G. Salamov* 2005 *J. Phys. D: Appl. Phys.* 38 682
- [13]. *M.M. Pejovic and R.D. Filipovic* 1989 *Int. J. Electron.* 67 251
- [14]. *C. Strumpel, Y.A. Astrov. and H.G. Purwins* 2002 *Phys. Rev. E* 65 066210
- [15]. *G. Vincent, D. Bois and A. Chantre* 1978 *J. Appl. Phys.* 53 3643
- [16]. *G. Vincent and D. Bois* 1978 *Solid State Commun.* 27 431
- [17]. *M.P. Shaw, V.V. Mitin, E. Schöll., and H.L. Grubin.,* *The Physics of Instabilities in Solid State Electron Devices* (Plenum, New York, 1992).
- [18]. *F.J. Niedernostheide* (ed.), *Nonlinear Dynamics and Pattern Formation in Semiconductors and Devices* (Springer, Berlin, 1995).
- [19]. *H.Y. Kurt, Y. Sadiq. and B.G. Salamov* 2008 *Phys. Stat. Sol. (a)* 205, N 2, 321
- [20]. *B. J. Clerjaud,* *Phys. C* 18, 3615 (1985).
- [21]. *M.M. Pejovic and G.S. Ristic,* 2002 *IEEE Transactions On Plasma Science,* 30, N3